

X-ray Crystallography and Magnetic Studies of a Stable Macrocyclic Tetranitroxide. Intramolecular Dimer of Nitroxides in a Constrained Geometry of the Upper Rim of Calix[4]arene

Andrzej Rajca,^{*,†} Maren Pink,[‡] Teerapat Rojsajakul,[†] Kan Lu,[†] Hua Wang,[†] and Suchada Rajca[†]

Contribution from the Department of Chemistry, University of Nebraska, Lincoln, Nebraska 68588-0304, and X-ray Crystallographic Laboratory, Department of Chemistry, University of Minnesota, Minneapolis, Minnesota 55455

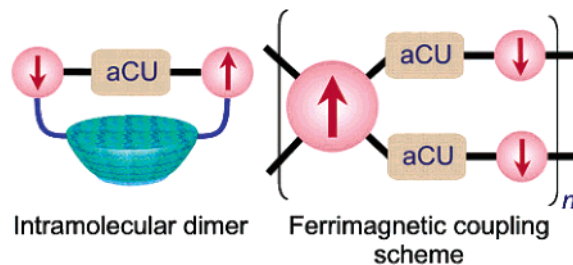
Received January 10, 2003; E-mail: arajca1@unl.edu

Abstract: Synthesis, crystallography, and magnetic characterization of a stable macrocyclic tetranitroxide **1**, a calix[4]arene, which is functionalized with four *tert*-butylnitroxides at the upper rim, is described. In solution, **1** has a 4-fold symmetric fixed cone conformation on the NMR time scale and small, but nonnegligible, exchange interactions between the radicals ($30\text{ K} > |J/k| \gg 1.8\text{ mK}$). In the solid state, dimerization of one diagonal pair of nitroxides leads to a pinched cone conformation for **1** with strong intradimer antiferromagnetic coupling with $|J/k| = 200\text{--}300\text{ K}$ (singlet–triplet energy gap, $\Delta E_{\text{ST}} \approx 1\text{ kcal/mol}$).

Introduction

Recent discovery of magnetic ordering in a conjugated organic polymer was based upon a rational design of connectivity between radicals, including the ferrimagnetic coupling scheme with antiferromagnetic coupling units (aCUs) mediating exchange coupling between unequal spins.^{1,2} With stronger and more reliable exchange couplings associated with such aCUs,^{3–5} higher ordering temperatures for such polymers may be feasible. It is well-known that intermolecular π -dimerization of nitroxides and other stable radicals may lead to relatively strong antiferromagnetic couplings.⁶ We envision that *intramolecular dimers* of stable di- and polynitroxides, with a conformationally restricted macrocyclic backbone, may provide novel aCUs. Such coupling units are essential for effective approaches to polymer-based organic magnets.¹

Intramolecular dimers may also serve as a model for dimerization of stable organic radicals in the solid state. For a number of such solids, interesting magnetic properties, including phase transitions with hysteresis of magnetic susceptibility vs temperature, were found.^{7–10} However, the rigorous X-ray



crystallographic and magnetic characterizations of dimers of stable organic radicals remain scarce and they are confined to intermolecular dimers of mono- and diradicals.^{6,11,12}

We report on the synthesis, X-ray crystallography, and magnetic measurements of the ambient stable nitroxide tetra-radical **1** based upon calix[4]arene, which is functionalized with four nitroxides at the upper rim.^{13,14} Dimerization of one diagonal pair of nitroxides leads to a pinched cone conformation of **1** in the solid state and strong intradimer antiferromagnetic coupling with $|J/k| = 200\text{--}300\text{ K}$ (singlet–triplet energy gap, $\Delta E_{\text{ST}} \approx 1\text{ kcal/mol}$).

Results and Discussion

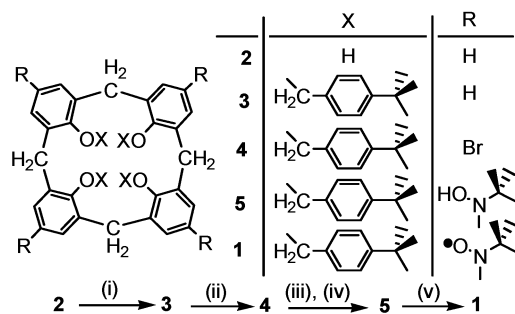
Synthesis. The synthesis of tetranitroxide **1** is outlined in Scheme 1. In the first step, the etherification of the lower rim

[†] University of Nebraska.

[‡] University of Minnesota. Present address: IUMSC, Department of Chemistry, Indiana University, Bloomington, IN 47405.

- (1) Rajca, A.; Wongsriratanakul, J.; Rajca, S. *Science* **2001**, *294*, 1503–1505.
- (2) Rajca, A.; Rajca, S.; Wongsriratanakul, J. *J. Am. Chem. Soc.* **1999**, *121*, 6308–6309.
- (3) Dougherty, D. A. *Acc. Chem. Res.* **1991**, *24*, 88–94.
- (4) Rajca, A. *Chem. Rev.* **1994**, *94*, 871–893.
- (5) Berson, J. A. *Acc. Chem. Res.* **1997**, *30*, 238–244.
- (6) Sakane, A.; Kumada, H.; Karasawa, S.; Koga, N.; Iwamura, H. *Inorg. Chem.* **2000**, *39*, 2891–2896.
- (7) Fujita, W.; Awaga, K. *Science* **1999**, *286*, 261–262.
- (8) Itkis, M. E.; Chi, X.; Cordes, A. W.; Haddon, R. C. *Science* **2002**, *296*, 1443–1445.
- (9) Sugano, T. *Polyhedron* **2001**, *20*, 1285–1289.
- (10) Postulated dimer of dinitroxides: Schultz, D. A.; Fico, R. M., Jr.; Boyle, P. D.; Kampf, J. W. *J. Am. Chem. Soc.* **2001**, *123*, 10403–10404.

- (11) Capiomont, P. A.; Chion, B.; Lajzerowicz, J. *Acta Crystallogr.* **1971**, *B27*, 322–326.
- (12) Fremy salt: Blackstock, S., personal communication. Howie, R. A.; Glasser, L. S. D.; Moser, W. *J. Chem. Soc. A* **1968**, 3043–3047.
- (13) Crystallography of tetranitroxides: Griesar, K.; Haase, W.; Svoboda, I.; Fuess, H. *Acta Crystallogr.* **1997**, *C53*, 1488–1490. Mathevet, F.; Luneau, D. *J. Am. Chem. Soc.* **2001**, *123*, 7465–7466 (as Mn(II) complex). Liao, Y.; Baskett, M.; Lahti, P. M.; Palacio, F. *Chem. Commun.* **2002**, 252–253.
- (14) Nitroxides and nitronyl nitroxides on the upper and lower rim of calix[4]arene, respectively: Wang, Q.; Li, Y.; Wu, G. *Chem. Commun.* **2002**, 1268–1269. Ulrich, G.; Turek, P.; Ziessel, R. *Tetrahedron Lett.* **1996**, *37*, 8755–8758.

Scheme 1. ^aSynthesis of Teranitroxide 1

^a Conditions: (i) NaH, THF/DMF, 4-*tert*-butylbenzylbromide, 40–56%; (ii) NBS, 2-butanone, 62–92%; (iii) *t*-BuLi (8 equiv), THF; (iv) [(CH₃)₃NO]₂ (2.1 equiv), 14–43% from 4; (v) Ag₂O, CHCl₃, 30–70%.

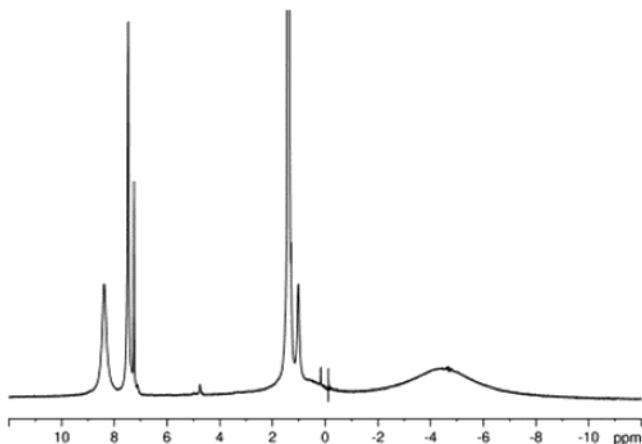


Figure 1. ¹H NMR (500 MHz) spectrum of **1** in CDCl₃ at 293 K. The tallest peak in the spectrum, the singlet at 1.40 ppm, is shown out of scale.

introduces a fixed cone conformation;¹⁵ both **3** and **4** show 4-fold symmetry on the ¹H (500 MHz) and ¹³C (125 MHz) NMR time scales at 295 K in CDCl₃. For tetrakis(hydroxyamine) **5**, only 2-fold symmetry on the ¹H NMR scale in CDCl₃ is found, as expected for a pinched cone conformation.¹⁶

Solution Studies of 1. ¹H NMR (500 MHz) spectra of **1** in CDCl₃ in the 298–223 K range are compatible with 4-fold symmetry. At 298 K, six broad resonances are observed; two 36-proton resonances at 1.40 and –4.5 ppm are assigned to the *tert*-butyl groups at the benzyl and nitroxide moieties, respectively (Figure 1). For the most downfield 8-proton ¹H resonances (8.39 and 7.48 ppm), which are tentatively assigned to the aromatic protons of the benzyl groups, the plots of observed frequency (V_{obs}) versus reciprocal temperature ($1/T$) give straight lines ($R = 0.999$ and 0.995).¹⁷ The bulk paramagnetic susceptibility (χ) measurements for **1** in 2-methyltetrahydrofuran (2-MeTHF) reveal a constant value of $\chi T \approx 1.3$ – 1.4 emu K mol^{–1} in the 290–30 K range.¹⁸ A similar value of $\chi T \approx 1.34 \pm 0.04$ (i.e., 3.57 ± 0.09 unpaired electrons per molecule) is obtained for **1** in chloroform using the ¹H NMR-based Evans method.¹⁹

(15) Gutsche, C. D.; Pagoria, P. F. *J. Org. Chem.* **1985**, *50*, 5795–5802.

(16) Pinched cone conformation for calix[4]arene with hydrogen-bonded groups on the upper rim: Conner, M.; Janout, V.; Regen, S. L. *J. Am. Chem. Soc.* **1991**, *113*, 9670–9671.

(17) For the two most downfield 8-proton ¹H resonances (8.39 and 7.48 ppm) and assuming four $S = 1/2$ radicals, numerical fitting of the observed frequency (V_{obs}) to $V_{\text{obs}} = V_{\text{dia}} + [4S(S+1)g\mu_B H_0(N_A) / (1 + (\gamma_N/2\pi)3kT)] = V_{\text{dia}} + 15.777A/T$, gives $V_{\text{dia}} = 3.0$ kHz, $A = 22$ kHz and $V_{\text{dia}} = 3.5$ kHz, $A = 3.5$ kHz, respectively. Reference 4 and *NMR of Paramagnetic Molecules*; La Mar, G. N., Horrocks, W. DeW., Jr., Holm, R. H., Eds.; Academic: New York, 1973.

(18) The low temperature (below 30 K) behavior of **1** will be reported separately.

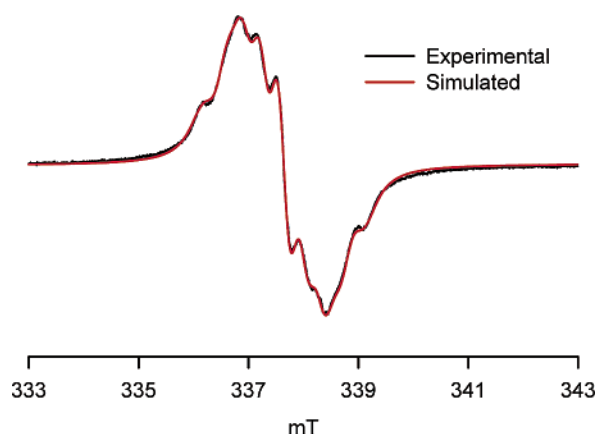


Figure 2. ESR (X-Band) spectrum of **1** in CDCl₃ at ambient temperature. Black trace: experimental spectrum. Red trace: numerical fit ($R = 0.999$) with the following variable parameters [rel concentration, Lorentzian line width, g -shift, ¹⁴N-splitting (spin, number), ¹H-splitting (spin, number)]: species no. 1 [77%, 0.285, –3.57, 0.328 (1, 4), 0.046 (0.5, 8)], species no. 2 [14%, 0.255, –3.40, 0.440 (1, 3), 0.058 (0.5, 6)], species no. 3 [9%, 0.265, –3.70, 0.690 (1, 2), 0.089 (0.5, 4)]. The line widths and hyperfine splittings are converted to milliTesla.

Therefore, the strength of exchange coupling between nitroxides in **1** in solution is well outside the 298–30 K range, providing an upper bound for $|J/k|$, i.e., $|J/k| < 30$ K.

ESR (X-band) spectra for **1** show detectable exchange coupling and provide the lower bound for $|J|$. At ambient temperature in CDCl₃, a poorly resolved multiplet ($g = 2.0058$) is obtained. The numerical fits ($R = 0.999$) reveal a mixture of oligonitroxides, containing about 75% of tetranitroxide **1** in addition to the corresponding tri- and dinitroxide impurities (Figure 2). A value of $\chi T \approx 1.37$ calculated for such a mixture is in excellent agreement with the magnetic susceptibility measurements. For **1** at ambient temperature, numerical fitting gives a nonet for the ¹⁴N hyperfine coupling with peak-to-peak splitting $H_{\text{pp}} \approx 0.328$ mT = $a_N/4$, i.e., $a_N = 1.31$ mT, which is in a good agreement with $a_N = 1.28$ mT for 3,5-dimethyl-4-methoxyphenyl-*tert*-butylnitroxide.²⁰ This is consistent with exchange-coupled nitroxides with a coupling constant significantly larger than the ¹⁴N hyperfine coupling, $|J/g\mu_B| \gg a_N$, i.e., $|J/k| \gg 1.8$ mK.

Both the smallness of the exchange coupling and the 4-fold symmetry on the NMR time scale are more consistent with the cone rather than pinched cone conformation for **1** in solution. Additional evidence in support of this finding is provided by the EPR spectroscopy of **1** in frozen 2-MeTHF at 77 K; the $\Delta m_s = 1$ region of the spectrum consists of several peaks spread over the spectral width ($|2D|$) of about 20 mT and the $\Delta m_s = 2$ signal is easily detectable. If **1** were in the pinched cone conformation, two of the diagonally positioned nitroxides would be in close proximity, leading to relatively large spectral width derived from their magnetic dipole–dipole interaction. According to a simple point-dipole approximation, $|2D| \approx 20$ mT corresponds to an effective distance of about 6 Å between the two magnetic dipoles.²¹ While the point-dipole approximation is not strictly applicable to **1**, delocalization of spin density into the relatively proximate benzene rings should even further

(19) Evans, D. F. *J. Chem. Soc.* **1959**, 2003–2005. Live, D. H.; Chan, S. I. *Anal. Chem.* **1970**, *42*, 791–792.

(20) Forrester, A. R.; Hepburn, S. P.; McConnachie, G. *J. Chem. Soc., Perkin Trans. I* **1974**, 2213–2219.

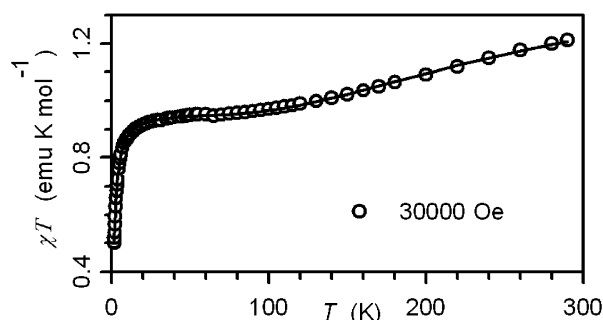


Figure 3. Plot of χT vs T for polycrystalline **1**. The numerical fit (solid line) to eq 1 has the following variable parameters (and their parameter dependencies): $J_1/k = -253$ K (0.90), $J_2/k = -1.5$ K (0.34), $N_1 = 0.649$ (0.88), $N_2 = 1.141$ (0.54); $R^2 = 0.9993$.

increase $|2D|$, compared to the case of localization of spin density on the NO moieties. For localized dinitroxides, in which the intramolecular distances between the midpoints of the N–O bonds were approximately 6.2 and 4.7 Å, $|2D| \approx 25$ mT and $|2D| \approx 40$ mT were measured.²²

Solid State Studies of 1. A plot of χT vs. T for the solid of **1** shows drastically different behavior compared to that found in solution (Figure 3). The high-temperature slope and low temperature downward turn in the χT vs T plot suggest the presence of strong ($|J/k| > 100$ K) and weak ($|J/k| < 10$ K) antiferromagnetic exchange interactions, respectively. When heating and cooling at various rates (≤ 2 K/min) within 2–300 and 90–370 K ranges, no hysteresis for χT vs T is detectable; only slow decomposition of **1** above 300 K is found.

To understand the origin of the strong exchange interactions in the solid state, the structure of **1** is determined by X-ray crystallography at 173 K (Figure 4).^{23a} One of the two pairs of diagonally positioned nitroxides is found in a parallelogram arrangement with close intramolecular contacts in the 2.6–2.8 Å range, well within the N–O van der Waals contact of 3.07 Å.²⁴ In this nitroxide dimer, the oxygens are disordered with occupancies of approximately two-thirds and one-third for the major (O2A and O2C) and minor (O2F and O2G) positions, respectively (Figure 4). The N–O bond lengths in this intramolecular dimer are elongated by 0.2–0.3 Å compared to those in the intermolecular dimers of nitroxides (and monomeric arylalkylnitroxides).^{6,11–13} These disorder affected, elongated N–O bond lengths may accommodate distortion to form the intramolecular dimer or be associated with hydroxyamines.²⁵ The latter, i.e., dimers of hydroxyamines, was explored in

alternative refinements but the results were inconclusive. It is also possible that crystal structure is of the solid solution type.

The molecules of **1** are packed as “bilayers” with the upper and lower rims of calix[4]arenes forming separate regions. Within each layer, the other, nondimerized, diagonally positioned pair of nitroxides in **1** is involved in short intermolecular contacts with the N···O distances of about 4.0 Å between the molecules translated along the b axis (Figure 5).²⁶

Another set of lesser quality X-ray crystallographic data on a different single crystal at 95 K (i.e., temperature near the plateau in the χT vs T plot) supports the structural findings at 173 K, except for small differences in disorder and methanol content.^{23b} The distances (and mutual orientations) of the nitroxide moieties in the intramolecular dimer and intermolecular close contacts in both structures are compatible with relatively strong and weak antiferromagnetic couplings, respectively.

Numerical fits to the χT vs T data (Figure 3) are based upon the model of two diradicals with variable number of molar equivalents (N_1 and N_2) and coupling constants (J_1/k and J_2/k), describing the intramolecular dimer and intermolecular N···O contacts in **1**, respectively (eq 1).

$$\chi T = (1.118T/H)[N_1F_1 + N_2F_2] \quad (1)$$

$$F_n = [2 \sinh(a)]/[1 + 2 \cosh(a) + \exp((-2J_n/k)/T)]; \quad n = 1, 2$$

$$a = 1.345(H/T)$$

Fitting with $N_1 \neq N_2$ indirectly accommodates tri- and dinitroxide impurities and other structures in which nitroxides are weakly coupled. The intradimer J_1/k has a substantial range (–200 to –300 K, 4 samples), which may in part have its origin in the variable occupancies for the crystallographically disordered major and minor positions of the nitroxide moieties of the dimer in polycrystalline samples used for magnetic measurements; the relatively shorter N···O contacts (and smaller N–O–N–O torsional angles) in the minor dimer are likely to be associated with stronger antiferromagnetic couplings.

The correlation between the magnetic data on 10-mg powder samples and structural data on single crystals is difficult; because of solvent loss, only broad powder diffraction patterns were obtained at room temperature. Therefore, a 0.5-mg batch of single crystals was selected under polarizing microscope. Following determination of full datasets for two crystals and cell constants for additional three crystals at 153 K (Table 1s, Supporting Information), the χT vs T plot, characteristic of tetranitroxide **1**, is obtained. These five datasets and the previously discussed dataset at 173 K possess essentially identical cell constants. (For the refined structures, small differences in methanol content were observed.) This suggests reproducibility of crystal structure for single crystals and, in conjunction with the high-temperature slope (and low temperature downward turn) in χT , confirms the presence of the intramolecular nitroxide dimer.

Conclusion

One pair of diagonal nitroxides on the calix[4]arene upper rim is found to form a strong antiferromagnetic, intramolecular

- (21) Eaton, S. S.; More, K. M.; Sawant, B. M.; Eaton, G. R. *J. Am. Chem. Soc.* **1983**, *105*, 6560–6567. The dependence of the spectral width ($|2D|$) on the inter-dipole distance (r) is calculated according to the following equation: $|2D| = 3g\beta/r^3 = 2.78 \times 10^3 (g/r^3)$, where $|D|$ is in mT and r is in Å. The $r = 5$ and 4 Å would correspond to $|2D|$ of about 40 and 80 mT, respectively, for a $g \approx 2$ diradical.
- (22) Rohde, O.; Van, S. P.; Kester, W. R.; Griffith, O. H. *J. Am. Chem. Soc.* **1974**, *96*, 5311–5318.
- (23) Crystallographic data for tetranitroxide **1**: (a) at 173 K (dataset A), $C_{88}H_{112}N_4O_8 \cdot 2.31CH_3OH$, red crystal ($0.17 \times 0.09 \times 0.04$ mm³), $T = 173$ K, triclinic, $P1$, $a = 10.2842(7)$ Å, $b = 13.0555(8)$ Å, $c = 33.167(2)$ Å, $\alpha = 95.779(1)^\circ$, $\beta = 96.733(1)^\circ$, $\gamma = 100.260(1)^\circ$, $V = 4318.0(5)$ Å³, $Z = 2$, $\mu = 0.071$ mm⁻¹, $R = 0.0640$, wR2 = 0.1680, GoF = 0.926 (F^2 , all data). (b) at 95 K (dataset B), $C_{88}H_{112}N_4O_8 \cdot 2CH_3OH$, orange crystal (cut, $0.05 \times 0.05 \times 0.005$ mm³), $T = 95$ K, triclinic, $P1$, $a = 10.260(2)$ Å, $b = 13.106(4)$ Å, $c = 32.814(11)$ Å, $\alpha = 95.487(9)^\circ$, $\beta = 90.497(15)^\circ$, $\gamma = 100.881(15)^\circ$, $V = 4311(2)$ Å³, $Z = 2$, $\mu = 0.045$ mm⁻¹, $R = 0.1253$, wR2 = 0.3164, GoF = 1.082 (F^2 , all data).
- (24) For intermolecular nitroxide dimers, typical N···O contacts and N–O bond lengths are 2.28–2.37 and 1.28 Å, respectively (refs 6, 11, 12).
- (25) Inoue, K.; Koga, N.; Iwamura, H. *J. Am. Chem. Soc.* **1991**, *113*, 9803–9810.

- (26) The oxygens of one of the nitroxides are also disordered over two positions (63:37) introducing the negligible difference of 0.03 Å for the two 4.0 Å N···O contacts; the N–O bond lengths are normal 1.28 Å.

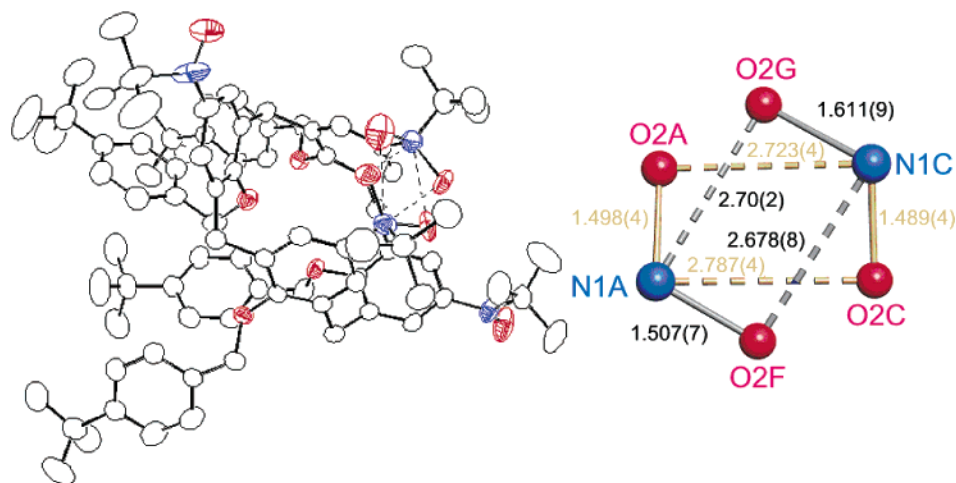


Figure 4. Molecular structure of **1** at 173 K. (A) Ortep plot (50% probability level). (B) N–O distances for the intramolecular dimer of nitroxides (major and minor occupancies); the O–N–O angles and the N–O–N–O torsions are in the 86.0–89.6° and 18.7–21.4° ranges, respectively.

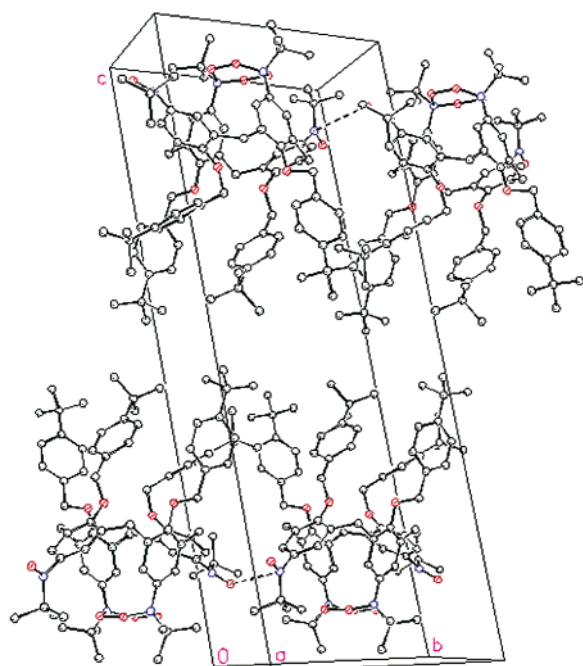


Figure 5. Crystal packing of **1** at 173 K, showing short intermolecular contacts with the N...O distances of about 4.0 Å. Hydrogen atoms and solvent molecules are omitted for clarity.

dimer in the solid state. Such intramolecular dimers of nitroxides may serve as antiferromagnetic coupling units, a promising building block for exchange-coupled macromolecules.

Experimental Section

5,11,17,23-Tetrakis(*N*-*tert*-butylhydroxyamine)-25,26,27,28-tetrakis(4'-*tert*-butylbenzyloxy)calix[4]arene (5**).** *t*-BuLi in pentane (3.7 mL, 6.0 mmol) was added to a tetrabromocalix[4]arene **4** (1.000 g, 0.755 mmol) in THF (25 mL) at -78°C . After 2 h at -78°C , 2-methyl-2-nitrosopropane dimer (0.3 g, 1.6 mmol) in THF (2 mL) was added. The reaction mixture was stirred for 30 min at -78°C and then allowed to warm to ambient temperature. After additional stirring for 3 h at ambient temperature, the orange reaction mixture was quenched with water (25 mL) and extracted with ether (2×25 mL). The organic layer was dried over MgSO_4 and evaporated to dryness. Column chromatography (25% ether in hexanes) and recrystallization from $\text{CHCl}_3/\text{MeOH}$ afforded an orange powder (0.446 g, 43%, mp = 188°C). From two reactions on the 1-g scale, 0.275 g (27%) and 0.143 g

(14%) of **5** were obtained. Anal. Calcd for $\text{C}_{88}\text{H}_{116}\text{N}_4\text{O}_8$: C, 77.83; H, 8.62. Found: C, 77.55; H, 8.31. ^1H NMR (500 MHz, CDCl_3): 8.873 (s, 2 H, exch D_2O), 7.476, 7.450 (AB, $J = 8.1$, 8 H), 7.041, 6.902 (AB, $J = 7.9$, 8 H), 7.002 (bs, 2 H), 6.865 (bs, 2 H), 6.370 (bs, 2 H), 6.00 (bs, 2 H, exch D_2O), 5.480 (bs, 2 H), 4.991 (s, 4 H), 4.67 (bs, 4 H), 4.239 (d, $J = 13.6$, 4 H), 3.01 (bd, $J = 14.1$, 2 H), 2.82 (bd, $J = 13.3$, 2 H), 1.347 (s, 9 H), 1.208 (s, 9 H), 1.170 (s, 9 H), 0.906 (s, 9 H). FABMS (3-NBA + Na^+): m/z (% RA in the m/z 1377–1386 range) at $(\text{M} + \text{Na})^+$, 1379.8 (100), 1380.8 (90), 1381.8 (48), 1382.8 (20); calcd for $\text{C}_{88}\text{H}_{116}\text{N}_4\text{O}_8\text{Na}_1$ 1379.87 (98), 1380.87 (100), 1381.88 (52), 1382.88 (18). IR (cm^{-1}): 3223, 2963, 2905, 2868, 1460, 1362, 1200.

5,11,17,23-Tetrakis(*N*-*tert*-butylaminoxyl)-25,26,27,28-tetrakis(4'-*tert*-butylbenzyloxy)calix[4]arene (1**).** Hydroxyamine **5** (150 mg, 0.11 mmol) in CHCl_3 (15 mL) was added to freshly prepared silver oxide (0.5 g). After stirring at room temperature in darkness for 18 h, the reaction mixture was filtered, and then the red filtrate was evaporated to dryness. Column chromatography (50% ether in hexanes) gave a red solid (126 mg). Recrystallization from MeOH gave red crystals (103 mg, 69%). From several reactions on the 100–200-mg scale, **1** was obtained in 30–70% isolated yields. Mp 130°C (under argon, dec). Anal. Calcd for $\text{C}_{88}\text{H}_{112}\text{N}_4\text{O}_8$: C, 78.06; H, 8.34. Found: C, 78.83; H, 8.39. ^1H NMR (500 MHz, CDCl_3 , ± 150 ppm, 295 K): 8.39 (bs, 8 H), 7.48 (bs, 8 H), 1.40 (s, 36 H), 1.02 (bs, ~ 8 H), 0.9 (br, ~ 8 H), -4.5 (br, 36 H). Evans method (4 measurements, $\text{CDCl}_3/\text{CHCl}_3$, 295 or 298 K), $\chi T = 1.3$ – 1.4 emu K mol^{-1} (3.5, 3.6, 3.6, 3.7 unpaired electrons). FABMS (3-NBA + Na^+): m/z (% RA in the m/z 1372–1386 range) at $(\text{M} + \text{Na})^+$, 1376.0 (74), 1376.9 (100), 1378.0 (70), 1378.0 (36); calcd for $\text{C}_{88}\text{H}_{112}\text{N}_4\text{O}_8\text{Na}_1$ 1375.84 (98), 1376.84 (100), 1377.84 (51), 1378.85 (15). IR (cm^{-1}): 2962, 1463, 1203, 977.

X-ray Crystallography for 1. Two datasets were collected: one on a Bruker SMART system at 173 K at the University of Minnesota (A) and the second at 95 K at beamline 15ID, ChemMatCARS, at the Advanced Photon Source, Argonne National Laboratory in Chicago (B). Final cell constants were calculated from the xyz centroids of strong reflections from the actual data collection after integration (SAINT). The intensity data were corrected for absorption (SADABS). The space group $P\bar{1}$ was determined on the basis of the lack of systematic absences and on intensity statistics. The structures were solved with direct-methods (SIR-92). Full-matrix least squares/difference Fourier cycles were performed (SHELXL-97). All non-hydrogen atoms were refined with anisotropic displacement parameters unless stated otherwise. All hydrogen atoms were placed in ideal positions and refined as riding atoms with relative isotropic displacement parameters.

Dataset A. A red plate ($0.17 \times 0.09 \times 0.04$ mm 3) obtained from a methanol solution by slow evaporation was selected for analysis. The data collection was carried out using Mo $\text{K}\alpha$ radiation (graphite

monochromator). All non-hydrogen atoms were refined with anisotropic displacement parameters, except for one partially occupied methanol molecule (O4E, C24E). The final full matrix least squares refinement converged to $R1 = 0.0640$ ($I > 2\sigma(I)$) and $wR2 = 0.1994$ (F^2 , all data). The remaining electron density is located in the vicinity of the disordered methanol molecules.

There are several incidents of disorder in the structure. First, the nitroxide dimer (having a parallelogram arrangement) is composed of two NO groups with oxygen atoms disordered over two positions (67:33). Alternative arrangements of the NO-dimer were considered (e.g., oxygen atoms interacting with each other). However, in a test calculation the site occupancies were refined independently from each other and resulted also in values of approximately two-thirds for O2A and O2C and one-third for O2F and O2G. No constraints were applied to any involved distances although it appears that the N–O distances are about 0.2 Å longer than expected and found for the NO groups B and D (approximately 1.28 Å). Second, another NO group is disordered over two positions (N1D/N1E). The corresponding *N*-bound *tert*-butyl group is disordered with 1.31 methanol molecules (O4D, C24D; O4E, C24E; O5, C25). The methanol molecule O5, C25 is further disordered over an inversion center and was refined with a partial site occupancy considering both the inversion center and the disorder with the *tert*-butyl group. Last, two of the *tert*-butyl groups connected to the phenyl rings of the upper rim are disordered over two sites. Similarly, the displacement parameters for the carbon atoms of a third *tert*-butyl group (C19D, C20D, C21D, C22D) are rather large. However, attempts to refine disorder failed; no definite second site was found.

Dataset B. An orange needle ($0.05 \times 0.05 \times 0.005$ mm³) obtained from a methanol solution by slow evaporation was selected for analysis at 95 K. The measurements were carried out using a Kappa SMART diffractometer equipped with a two by two array of 1K CCD detectors and a wavelength of 0.55942 (~Ag K α). All non-hydrogen atoms were refined with anisotropic displacement parameters with the exception of the carbon and oxygen atoms of the disordered solvent molecules. The final full matrix least squares refinement converged to $R1 = 0.1253$ and $wR2 = 0.3361$ (F^2 , all data). The remaining electron density is located in the vicinity of the disordered methanol molecules. The structure is similar to A, varying in site occupancies of the nitroxide moieties (73:27 for the intramolecular nitroxide dimer) and solvent content.

As a test for the alternative dimer of hydroxylamines structure, refinement of dataset A was carried out using idealized OH group with a tetrahedral N–O–H angle. The hydrogen was allowed to rotate about the N–O bond; this motion was combined with the riding motion of the H atom on its parent atom. Unreasonable displacement parameters for the hydrogens were obtained, probably due to the vicinity of the hydrogens to the disordered oxygen atoms. This result still does not preclude the solid solution type of crystal structures.

Magnetic Studies. The sample vessels for the SQUID measurements were based upon 5-mm OD EPR-quality quartz tubes (Wilmad), modified to possess a thin bottom, which is 6 cm from the end of the tube. This geometry allows for an approximate offset of the diamagnetic background above and below the bottom of the tube. For solution

samples, the tetranitroxide (0.5–2 mg) was loaded to the tube, solvent was vacuum transferred to form ca. 5-mm high band of solution of tetranitroxide, and then the tube was flame sealed under vacuum. The tubes were inserted to MPMS55 SQUID magnetometer at near the room temperature (290–300 K); the initial sequence of measurements was in the cooling mode to allow for condensation of the solvent. For solid-state samples, the tetranitroxide was loaded to the tube, placed under vacuum, and then flame sealed under partial pressure of helium gas (about 100 mTorr). The sample tubes were stored in liquid nitrogen.

The magnetic data were corrected for diamagnetism as follows. For solution samples, the χ vs $1/T$ plots were extrapolated from the $T = 100$ – 240 K range (cooling mode of the MPMS55). For solid samples, the tetranitroxide was removed from the sample tube, and then each empty tube was subjected to the identical sequence of measurements as the original sample. After the point-by-point correction with these data, the molar susceptibilities were further corrected using the Pascal constants (-9.24×10^{-3} emu mol⁻¹).

Correlation between the Structural and Magnetic Data. A batch of single crystals (0.5 mg) is selected under a polarizing microscope. Datasets for two crystals and cell constants for three crystals at 153 K are determined and compared to the dataset A (Table 1s, Supporting Information).

Following single crystal determination of cell constants as described above, the 0.5-mg batch of single crystals of tetranitroxide was loaded to a gelatine capsule. Due to the unknown amount of diamagnetic oil, used for mounting of crystals in diffractometer, only qualitative magnetic data could be obtained.

Acknowledgment. This research was supported by the National Science Foundation grants to A.R. (CHE-9806954 and CHE-0107241). MS analyses were carried out at the Nebraska Center for Mass Spectrometry. ChemMatCARS Sector 15 is principally supported by the National Science Foundation/Department of Energy under Grant CHE0087817 and by the Illinois Board of Higher Education. The Advanced Photon Source is supported by the U.S. Department of Energy, Basic Energy Sciences, Office of Science, under Contract W-31-109-Eng-38. We thank Professor Silas Blackstock for providing us with the new crystallographic data on Fremy salt. We thank Dr. Makoto Miyasaka and Jirawat Wongsriratanakul for growing additional crystals of **1** and assistance with magnetic measurements.

Supporting Information Available: Experimental section (synthetic details for compounds **3** and **4**, materials, special procedures, instrumentation, numerical fitting), ESR spectrum for **1** at 77 K, summary of cell constants, and X-ray crystallographic files (datasets A and B in CIF format). This material is available free of charge via the Internet at <http://pubs.acs.org>.

JA034115P